The analysis of particle number densities in dilute gas-particle flows: the Eulerian and Lagrangian methods

A. K. Gilfanov,[1,*] T. S. Zaripov,[2,] S. S. Sazhin,[2,***] and O. Rybdylova[2,****]**

(Submitted by A. M. Elizarov)

[1] *N.I. Lobachevsky Institute of Mathematics and Mechanics, Kazan (Volga Region) Federal University, Kremlevskaya ul. 18, Kazan, Tatarstan, 420008 Russia*
[2] *Advanced Engineering Centre, School of Architecture, Technology and Engineering, University of Brighton, Brighton, BN2 4GJ, UK*

Received XXX; revised XXX; accepted XXX

Abstract—The predictions of the conditional quadrature methods of moments, conventional Lagrangian, and fully Lagrangian (FLA) approaches to the calculation of particle number densities in hyperbolic and Lamb vortex flows are compared. All these methods predict similar distributions of particle number densities at low Stokes numbers. For single-fold particle trajectory crossings (PTC) at high Stokes numbers in the hyperbolic flow, the two-point quadrature approximation is shown to be in good agreement with both Lagrangian approaches, while the three-point approximation of the VDF leads to worse prediction than the two-point approximation. Thus, the number of nodes in the approximation has to be chosen based on the characteristics of the flow. The predictions of the FLA are shown to agree with those of the conventional Lagrangian approach when sufficiently large numbers of particles are used in calculations. The FLA is shown to be the most CPU efficient method among those considered in our analysis.

2010 Mathematical Subject Classification: 70-08

Keywords and phrases: *dilute gas-particle flow, inertial particles, particle trajectory crossings, conditional quadrature method of moments, fully Lagrangian approach*

1. INTRODUCTION

Mathematical modelling of dilute gas-particle flows has been used in many applications, including those of mechanical and chemical engineering [9, 10]. Particles are commonly assumed to be fine, with velocities equal to that of the gas phase so that their trajectories follow the streamlines of the carrier phase. This approximation is not valid for heavy particles whose velocities might differ from local gas velocities (e.g. fuel droplets during pulse injections in internal combustion engines [9] and aerosol sampling [16]). In this case the particle Stokes number may not be small, and the particles need to be considered as inertial. When particles are inertial and free transport of particles prevails over collisions between them the particle trajectory crossing (PTC) can occur. The PTCs are characterised by the presence of particles with different velocities in the same point of space. One can distinguish between a homo-PTC problem, which considers trajectory crossings of particles of the same size, and a hetero-PTC problem, dealing with trajectory crossings of particles of different sizes [7]. A number of Eulerian-Eulerian and Eulerian-Lagrangian approaches have been developed for the analysis of these problems [3, 12, 13].

Within the traditional Lagrangian approach the particle number density is calculated based on direct counting of particles in individual cells, which requires an excessively large number of

* E-mail: Artur.Gilfanov@kpfu.ru
** E-mail: T.Zaripov2@brighton.ac.uk
*** E-mail: S.Sazhin@brighton.ac.uk
**** E-mail: O.Rybdylova@brighton.ac.uk

trajectories to be considered [3]. A more efficient approach to its calculation was suggested by Osiptsov [23, 24]. The latter approach is based on the continuity equation for particles in the Lagrangian form, and the Jacobi matrix of the Eulerian-Lagrangian transformation for calculating particle number density along trajectories. This is commonly known as the fully Lagrangian approach (FLA). Benefits of the FLA were demonstrated by Healy and Young [17], Zaripov et al. [29], Papoutsakis [25] and Li [21].

An alternative Eulerian approach to modelling gas-particle flows is based on solving transport equations for dispersed and continuous phases and the coupling between them, taking into account the polydispersity of particles in the general case. One possible simplification of this approach is based on the assumption that particles are of the same size (monodisperse) and have the same velocity (monokinetic) at a given point in space (possible contributions of folds are not taken into account). In this case, the dispersed phase is modelled as a fluid with an equilibrium velocity, and pressureless gas dynamic-like equations are solved. This approach cannot consider particle trajectory crossings as these crossings produce delta-shocks in regions with PTC [4, 5, 8]. To account for the polydispersity of particles, the multifluid model was introduced [19]. In this model, the range of particle sizes is split into sections, and transport equations for particles are solved under the assumption that each section is characterised by its own particle number density and momentum. This approach allows us to study hetero-PTC, but not homo-PTC.

For treating the homo-PTC problems a number of approaches were developed based on the solution the Boltzmann-Williams kinetic equation [26] by quadrature methods of moments (QMOM) [6, 11, 22, 27]. In such approaches the kinetic equation written for a number density function (NDF), with respect to sizes and velocities of particles, is transformed to the transport equation for NDF moments using the NDF representation in the form of weighted sum of various kernel functions (the Dirac delta functions in the original QMOM). In [6], the two-node QMOM was applied to the analysis of a velocity distribution function (VDF), and it was shown that using a two-node quadrature in the VDF representation allows one to resolve homo-PTC. The version of the quadrature method of moments developed by Fox [11] complemented the multifluid approach [4, 5, 18]. It was used to simulate evaporating sprays and both homo- and hetero-PTCs. The conditional quadrature method of moments (CQMOM) was proposed in [27] to describe the dynamic of a multivariate NDF using arbitrary numbers of quadrature nodes. Gilfanov et al. [15] modified the moment inversion algorithm on the QMOM and CQMOM in order to guarantee bounded particle velocities in the VDF representation that increased stability of the method.

Laurent et al. [20] reviewed state-of-the-art Eulerian approaches to simulate flows with PTC. The CQMOM was compared to the multi-Gaussian (MG) approach [1], in which the NDF is approximated using the Gaussian function instead of the Dirac delta function. It was shown that, for homogeneous isotropic turbulence, predictions of the MG are in better agreement with those of the Lagrangian approach than with those of the CQMOM. The extended quadrature methods of moments (EQMOM) [28] were developed based on the CQMOM and MG approaches. In these methods, continuous kernel functions with a different kind of support were used. A generalisation of EQMOM with Gaussian kernel functions was developed by Chalons et al. [2]. In methods of moments with continuous approximation, however, discrete representation of the NDF is lost. This perpetuates interest in the development of methods with a discrete form of the NDF, such as CQMOM. The promising approach known as the conditional hyperbolic quadrature method of moments (CHyQMOM) was proposed by Fox et al. [14]. CHyQMOM uses a lower number of moments, fixing the highest moment, so that the system of moment advection equations becomes hyperbolic.

In this work we compare predictions of previously proposed modification of CQMOM [15] with those of the traditional Lagrangian (box counting) and fully Lagrangian approaches for the analysis of particle number densities in hyperbolic and Lamb vortex flows (two-dimensional fluid flow fields with possible PTC). The adequacy of the PTC representation produced by the CQMOM with different numbers of quadrature nodes in the NDF approximation is assessed.

2. LAGRANGIAN APPROACHES

2.1. The conventional Lagrangian approach (box counting)

In the two-dimensional case, the motion of a single particle in a gas flow, taking into account Stokes' law of aerodynamic drag, is described by the following equations for the dimensionless coordinates (x, y) and dimensionless velocity components (u, v) of a particle,

$$\frac{du}{dt} = \frac{u_g - u}{\mathrm{Stk}}, \frac{dv}{dt} = \frac{v_g - v}{\mathrm{Stk}}, \frac{dx}{dt} = u, \frac{dy}{dt} = v, \tag{1}$$

where (u_g, v_g) is the gas velocity, and Stk is the Stokes number.

For the calculation of particle number densities on a uniform Eulerian computational grid, including many rectangular cells, N_p particles are initially placed in each cell and their trajectories are tracked. At each time step, the normalised particle number density in each cell is estimated along with the ratio of the number of particles in the cell to N_p. The accuracy of the method depends on grid resolution and the value of N_p. Hereafter, we will refer to this method as box counting [25] and the relevant particle number density is referred to as n_{BC}. Box counting will be used as the reference solution. The predictions of other methods will be assessed against the predictions of the method based on box counting.

2.2. The fully Lagrangian approach (FLA)

The fully Lagrangian approach (FLA) [23, 24] allows us to compute the particle number density n along a particle trajectory. The continuity equation in the Lagrangian form is written as

$$n(x_0, y_0, t)|det\,\|J\|\,| = n(x_0, y_0, 0), \tag{2}$$

where (x_0, y_0) is the initial position of a particle, J is the Jacobi matrix of the Eulerian-Lagrangian coordinate transformation. In the two-dimensional case, the components of the Jacobi matrix are defined as

$$J_{11} = \frac{dx}{dx_0}, J_{12} = \frac{dx}{dy_0}, J_{21} = \frac{dy}{dx_0}, J_{22} = \frac{dy}{dy_0}.$$

To calculate the values of the components of J, the following system of ordinary differential equations for J_{ij} and auxiliary variables ω_{ij} is solved along each trajectory:

$$\frac{dJ_{11}}{dt} = \omega_{11}, \frac{dJ_{12}}{dt} = \omega_{12}, \frac{dJ_{21}}{dt} = \omega_{21}, \frac{dJ_{22}}{dt} = \omega_{22},$$

$$\frac{\omega_{11}}{dt} = \frac{1}{\mathrm{Stk}}\left(J_{11}\frac{\partial u_g}{\partial x} + J_{21}\frac{\partial u_g}{\partial y} - \omega_{11}\right), \frac{\omega_{12}}{dt} = \frac{1}{\mathrm{Stk}}\left(J_{12}\frac{\partial u_g}{\partial x} + J_{22}\frac{\partial u_g}{\partial y} - \omega_{12}\right),$$
$$\frac{\omega_{21}}{dt} = \frac{1}{\mathrm{Stk}}\left(J_{11}\frac{\partial v_g}{\partial x} + J_{21}\frac{\partial v_g}{\partial y} - \omega_{21}\right), \frac{\omega_{22}}{dt} = \frac{1}{\mathrm{Stk}}\left(J_{12}\frac{\partial v_g}{\partial x} + J_{22}\frac{\partial v_g}{\partial y} - \omega_{22}\right).$$

The initial conditions for the Jacobian components are set as $J_{11} = 1, J_{12} = 0, J_{21} = 0, J_{22} = 1$ (at the starting point, Lagrangian and Eulerian coordinates are the same). Assuming that all particles start with the same initial velocity, the initial values of ω_{ij} are set to zero. When the values of the components of the Jacobian are found, the particle number density can be calculated from Eq. (2).

In the FLA, PTC can be detected by following a single trajectory: the value of the determinant of the Jacobi matrix crosses zero (changes sign) when PTC occurs. Due to this fact, a special treatment is required to translate the particle number density, calculated along the particle trajectory using the FLA, to the Eulerian grid. Consider a set of particles representing a single cloud, continuous in space at the initial time instant. If no PTC has occurred, the particle number density in cell n_{FLA} at a given time instant is equal to the particle number densities averaged over all particles in the cell. If PTC has occurred only for some particles in the cell (possibly more than once), then particles are grouped by the number of times the determinant of their Jacobi matrixes has crossed zero (the number of folds). In this case, n_{FLA} in the cell is calculated as a sum of particle number densities, averaged over each group.

3. METHOD OF MOMENTS

In the Eulerian framework to model particle transport the conditional quadrature method of moments (CQMOM) is used. This method is based on the kinetic equation which in the two-dimensional case has the following form

$$\frac{\partial f}{\partial t} + u\frac{\partial f}{\partial x} + v\frac{\partial f}{\partial y} + \frac{\partial (A_x f)}{\partial u} + \frac{\partial (A_y f)}{\partial v} = 0, \tag{3}$$

where $f(t, x, y, u, v)$ is the bivariate velocity distribution function, (A_x, A_y) are the components of the Stokes drag force (the first two equations in Eq. (1)).

The moments of $f(t, x, y, u, v)$ are defined as

$$M_{m,n}(t, x, y) = \int_{-\infty}^{\infty}\int_{-\infty}^{\infty} u^m v^n f(t, x, y, u, v) du dv. \tag{4}$$

Integrating Eq. (3) over velocity space and using (4) leads to the system of moment transport equations

$$\frac{\partial M_{m,n}}{\partial t} + \frac{\partial M_{m+1,n}}{\partial x} + \frac{\partial M_{m,n+1}}{\partial y} = \frac{u_g M_{m-1,n} - M_{m,n}}{\mathrm{Stk}} m\theta(m) + \frac{v_g M_{m,n-1} - M_{m,n}}{\mathrm{Stk}} n\theta(n), \tag{5}$$

where

$$\theta(x) = \begin{cases} 0, x \le 0 \\ 1, x > 0 \end{cases}.$$

To close flux term in (5) we use the CQMOM approximation for VDF at time t and point (x, y) in the following form

$$f(u, v) = \sum_{i=1}^{N_1}\sum_{j=1}^{N_2} w_{ij}\delta(u - u_i)\delta(v - v_{ij}), \tag{6}$$

where N_1 and N_2 are numbers of quadrature points in u- and v-velocity spaces, respectively, w_{ij} are the weights of nodes, u_i are abscissas in the u-velocity space, and v_{ij} are abscissas in the v-velocity space for given u_i. Such an approximation leads to an arbitrary moment

$$M_{m,n} = \sum_{i=1}^{N_1}\sum_{j=1}^{N_2} w_{ij} u_i^m v_{ij}^n.$$

The number of moments in (5) is inferred from the number of quadrature points in each direction: N_1 and N_2. As in [15] three cases are considered:

1. $N_1 = 1, N_2 = 1$: 1 node, 3 moments;
2. $N_1 = 2, N_2 = 2$: 4 nodes, 10 moments;
3. $N_1 = 3, N_2 = 3$: 9 nodes, 21 moments.

Zeroth moment M_{00} corresponds to the particle number density. Cases a, b, c are referred to as the one-point (MOM-1), two-point (MOM-2) and three-point (MOM-3) quadrature approximations, respectively. Hereafter, notations n_{MOM-1}, n_{MOM-2} and n_{MOM-3} are used for number density obtained for these cases.

To solve system of Eqs. (5) the previously proposed computational scheme is used [15]. This scheme applies the moment inversion algorithm with controlling boundedness of abscissas in the VDF representation (6). A source term is accounted for during a separate step using the operator-splitting technique. For example, the drag force for particles is accounted for using the analytical solution for particle velocities (see Eq. (1)), as in [6]. Assuming constant gas velocity during the time step $[t, t + \Delta t]$, the expression for u-velocity is presented as:

$$u(t + \Delta t) = u_g - (u_g - u(t)) \exp(-\Delta t/\mathrm{Stk}).$$

4. NUMERICAL RESULTS

4.1. Hyperbolic flow

In the general case, PTC can occur inside a single cloud due to the inertial behaviour of particles when the velocity of the carrier phase changes its direction. Consider an analytical model of colliding jets: a hyperbolic flow with the velocity components $u_g = x, v_g = -y$. The streamlines of the fluid flow in the computational domain $(-1 < x < 0, -1 < y < 1)$ are shown in Fig. 1. Particles with $\mathrm{Stk} = 0.25$ and $\mathrm{Stk} = 1$ are injected with a dimensionless y-component of velocity equal to 1 at the bottom boundary $y = -1$ at $-0.1 < x < -0.01$.

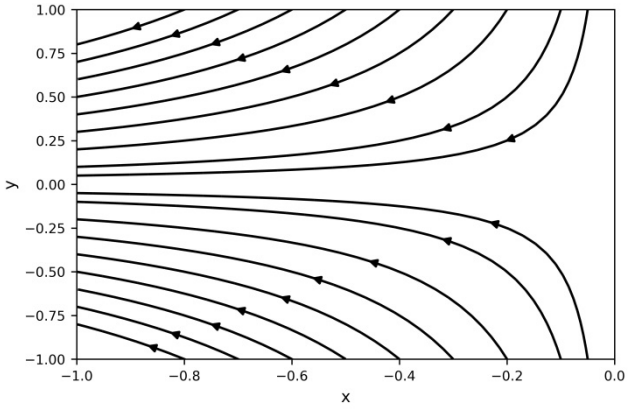

Figure 1. Streamlines of a hyperbolic flow.

CQMOM calculations (MOM-1, MOM-2, MOM-3) were performed on a uniform rectangular grid of 512×1024 points using an explicit first order scheme and a quasi-second order scheme in the physical space. In the cells where particles are injected, their number density and velocity were set equal to 1. At all other boundary cells, particle number density and velocity were set equal to zero. On the right boundary (see Fig. 1), a zero flux condition was used. Boundary conditions for the moments were calculated using the values of particle number density and velocity.

For Lagrangian calculations (box counting, FLA), particles were initialised in the same injection cells that were used for the CQMOM. In the case of Lagrangian box counting, each injection cell was uniformly populated with 16384 (128×128) particles (1.5×10^9 particles overall). In the case of the FLA, 1024 particles were placed in the injection region. The number densities predicted by these methods were projected to the Eulerian grid.

The distributions of number densities of low inertia particles with $\mathrm{Stk} = 0.25$, obtained using Lagrangian box counting, the FLA, and three versions of the CQMOM are shown in Fig. 2. As follows from this figure, the clouds do not cross the line $y = 0$ and no PTC occurs. In the absence of PTC, all methods predict qualitatively similar results: number densities grow in the accumulation region near the line $y = 0$.

The particle number density distributions along the vertical lines $x = -0.4$, $x = -0.2$ and $x = -0.1$, predicted by these approaches, are shown in Fig. 3. All three versions of the CQMOM predict non-zero concentration above the line $y = 0$, while both Lagrangian methods predict that no particles cross this line. The CQMOM approaches underestimate the maxima of particle number density compared to the Lagrangian approaches. Predictions by the FLA and box counting are almost identical until the particle number densities reach their maxima. The one-point quadrature approximation (MOM-1) predicts the maximum particle number density that is closest to the one inferred from the Lagrangian approach. The highest values of particle number density are $n_{FLA} = 13.55$, $n_{BC} = 10.6$, $n_{MOM-1} = 7.4$, $n_{MOM-2} = 6.8$, $n_{MOM-3} = 6.9$.

The distributions of number densities of high inertia particles with $\mathrm{Stk} = 1$, calculated using Lagrangian box counting, FLA and three versions of the CQMOM, are shown in Fig. 4. As follows from this figure, the particles cross axis $y = 0$, but due to the reverse fluid flow their trajectories turn back near the line $y = 0.3$. This leads to formation of a wide region with particle trajectory crossings.

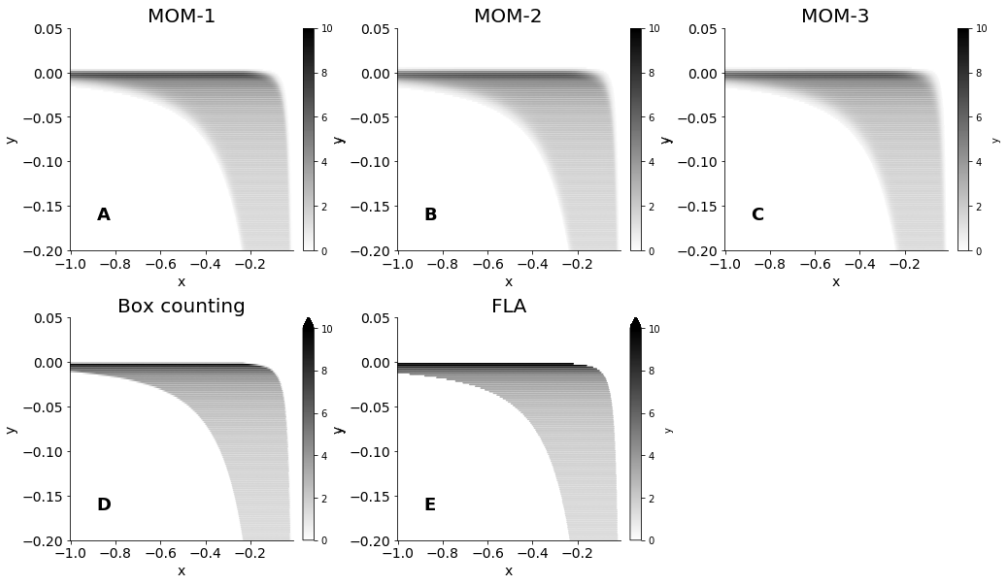

Figure 2. The distribution of the number density of particles with Stk = 0.25 in a hyperbolic flow. The number density was calculated using MOM-1 (A), MOM-2 (B), MOM-3 (C), box counting (D) and FLA (E).

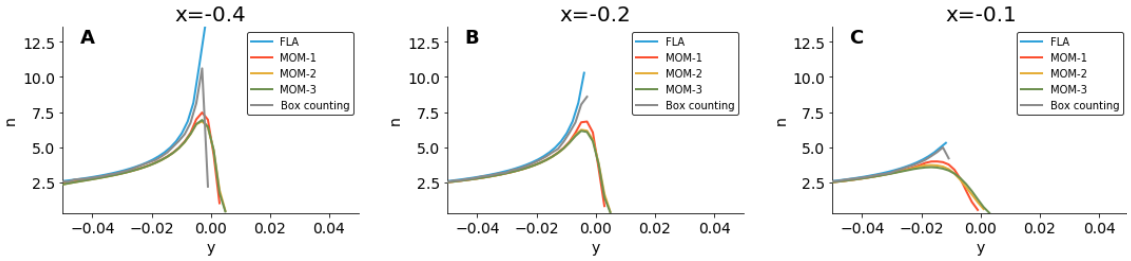

Figure 3. The number density of particles with Stk = 0.25 in the hyperbolic flow along lines $x = -0.4$ (A), $x = -0.2$ (B) and $x = -0.1$ (C).

The particle number densities along lines $x = -0.4$, $x = -0.2$ and $x = -0.1$ are shown in Fig. 5. As follows from this figure, the predictions of both Lagrangian approaches are rather similar. For example, a step-like increase in calculated number density due to the contribution of a reversed particle flow at $y = 0.17$ (Fig. 5(B)) and $y = 0.1$ (Fig. 5(C)) can be clearly seen. Note, however, that at y greater than 0.3 the particle number density predicted by box counting reaches its maximum value and drops sharply after that, while the density predicted by the FLA tends to infinity at these values of y.

As follows from Figs. 4 and 5, the one-point quadrature approximation predicts the collapse of the cloud at the PTC region and consequent growth of particle number densities to much higher values than predicted by MOM-2, MOM-3 and even box counting. Note that calculations based on the two-point quadrature approximation (MOM-2) show the best agreement with those based on both Lagrangian approaches. These calculations predict similar particle clouds and similar locations for the maxima of these densities at the trajectory-turning region (Fig. 4 (B), Fig. 5 (B, C)). Note, however, that MOM-2 has an unphysical jump in particle number density at $y = 0.14$ where the cloud meets its returning front.

Calculations based on the three-point quadrature approximation (MOM-3) and those based on the Lagrangian approaches predict similar locations where the cloud meets its returning front, and similar values for the particle number densities at these locations (Fig. 5 (B, C)). The predicted distribution of n_{MOM-3}, however, has many local unphysical jumps in particle number density (Fig. 4 (C)). The locations of nMOM-3 maxima are close to those of n_{MOM-1}, which can be attributed to the fact that the weight of the central quadrature node is high.

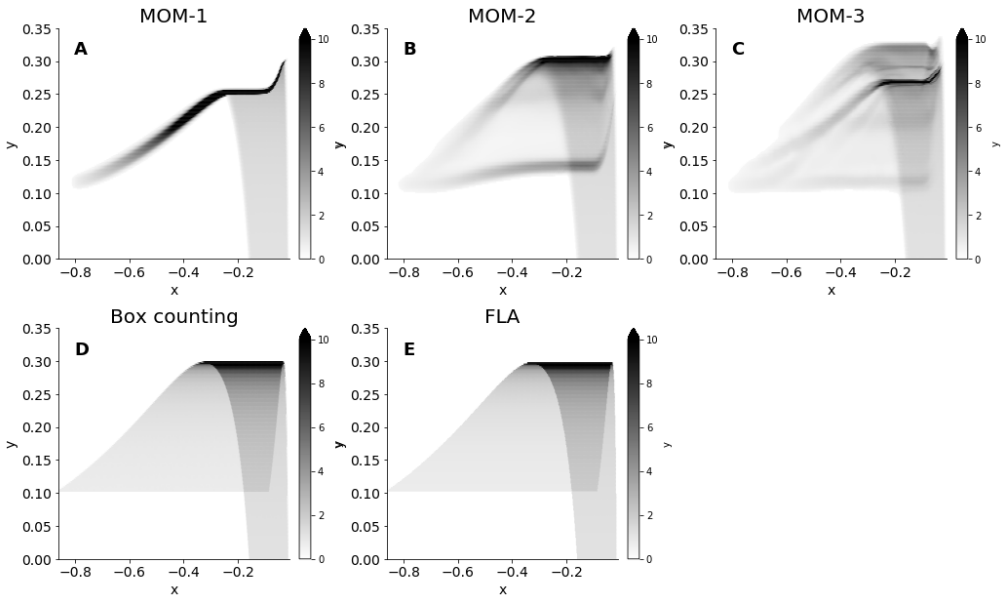

Figure 4. The distributions of number densities of particles with Stk = 1 in the hyperbolic flow, calculated using MOM-1 (A), MOM-2 (B), MOM-3 (C), box counting (D) and the FLA (E).

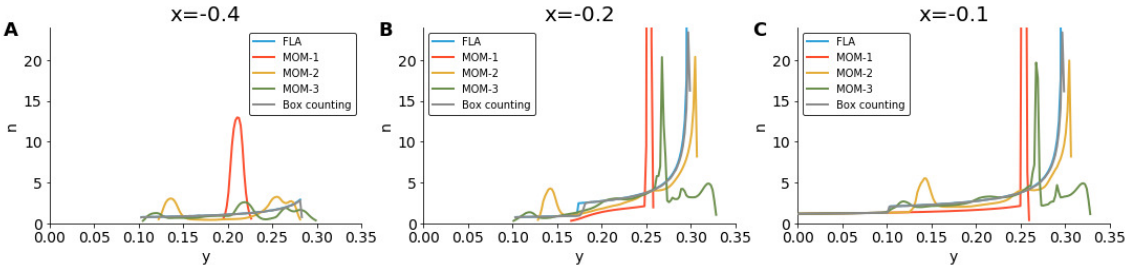

Figure 5. The number densities of particles with Stk = 1 in the hyperbolic flow along lines $x = -0.4$ (A), $x = -0.2$ (B) and $x = -0.1$ (C).

Note that, for Stk = 1, the conventional MOM calculations cannot be completed without ensuring that abscissas are in the physically allowable range. This is because very high value abscissas cause a significant reduction in time step. The numerical scheme using the new criterion was free from such time step related issues.

Calculations using the above-mentioned approaches were performed on an eight-core personal computer in parallel mode. The three-point quadrature approximation (MOM-3) required much more calculation time than MOM-1 and MOM-2. In the case of a single hyperbolic flow, calculations for 4 seconds of simulation time took about 20 minutes when MOM-1 was used. The MOM-2 calculations required about 2.5 hours for the same case (this involved the time-consuming moment inversion algorithm). The MOM-3 calculations took about a day for the same problem. In the latter case, many more scalars were transported (21 moments), and the moment inversion algorithm was more complex than that of MOM-2. The computational time for the traditional Lagrangian approach was about 4 hours. This is much less than the time required for MOM-3 and comparable to that for MOM-2. The most efficient method for this case was the fully Lagrangian approach when the same calculations took just several minutes. This is attributed to the fact that only one particle in each cell was needed to calculate particle number density in it using the fully Lagrangian approach.

4.2. Lamb vortex flow

The Lamb vortex is a model of a vortex flow that has a motionless core and diffuses into its surroundings. The model is described by the exact analytical solution to the transient Navier–

Stokes equations:

$$(u_g, v_g) = \frac{(-y, x)}{2\pi r^2}\left(1 - \exp(-\mathrm{Re}\frac{r^2}{4t})\right),$$

where Re is the Reynolds number and $r = \sqrt{x^2 + y^2}$.

We considered the Lamb vortex flow with $\mathrm{Re} = 100$ in domain $-1 < x < 1, -1 < y < 1$. A uniform rectangular computational grid of 1024×1024 points was used for the CQMOM simulations based on an explicit first order scheme and a quasi-second order scheme in the physical space. The zero-flux condition was used for the moments at all boundaries of the computational domain. Particle number densities predicted by the Lagrangian box counting and FLA simulations were calculated on the same Eulerian grid. Particles with zero velocity were initialised inside the ring $0.01 < r < 0.1$. The domain $r < 0.01$ inside the ring was left empty due to the infinite gas velocity at the ring centre.

Initially motionless particles were entrained by the surrounding carrier phase spiral flow. Carrier phase velocity decreased both in time and along the radius leading to formation of the particle accumulation zone at the outer surface of the ring; no PTCs occurred for this flow. Average radial profiles of particle number density, obtained using both Lagrangian methods and CQMOM at different time instants, are shown in Figs. 6 and 7 for $\mathrm{Stk} = 0.25$ and 1, respectively.

For $\mathrm{Stk} = 0.25$, FLA and Lagrangian box counting led to predictions of two accumulation zones at an early stage (two peaks in Fig. 6 (A), $t = 0.4$). This can be attributed to the fact that particles starting closer to the interior boundary of the initial ring reach higher velocities and catch up with particles at the outer surface of the ring. Eventually, these accumulation zones merge into one, leading to the formation of a narrow ring (Fig. 6(B, C), $t = 0.8, 1.2$). This effect was not captured by any of the CQMOMs.

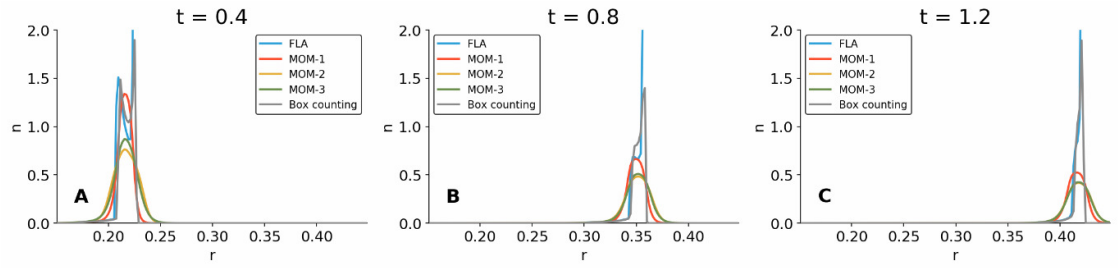

Figure 6. Averaged radial particle number density profiles for $\mathrm{Stk} = 0.25$ in a Lamb vortex flow at time instants $t = 0.4$ (A), $t = 0.8$ (B), $t = 1.2$ (C).

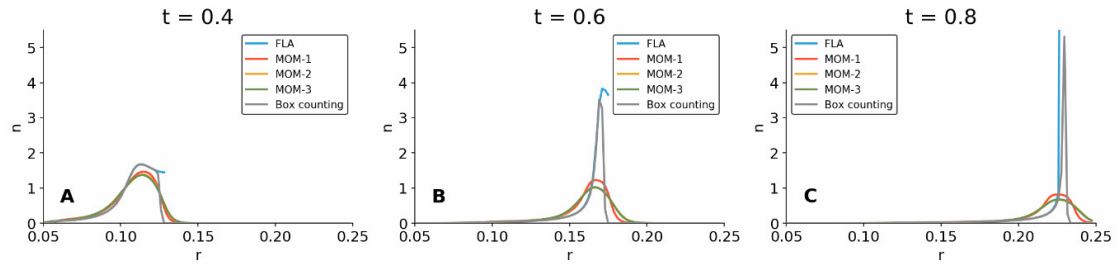

Figure 7. Averaged radial particle number density profiles for $\mathrm{Stk} = 1$ in a Lamb vortex flow at time instants $t = 0.4$ (A), $t = 0.6$ (B), $t = 0.8$ (C).

For $\mathrm{Stk} = 1$, the cloud expands more slowly than in the case of $\mathrm{Stk} = 0.25$. For Lagrangian calculations, the formation of two accumulation zones was not observed, although the number density around $x = 0.12$ tends to flatten (see Fig. 7(A)). As in the case of $\mathrm{Stk} = 0.25$, both Lagrangian approaches predict narrowing of the cloud with time with a very sharp drop in the

number density at the outer edge. For both $\mathrm{Stk} = 0.25$ and $\mathrm{Stk} = 1$, all CQMOMs predict wider rings with lower values of number density maxima, compared with those inferred from calculations based on the Lagrangian approaches. Also, these particle number density maxima, predicted based on the CQMOMs, decreased with time in contrast to those predicted using both Lagrangian approaches.

In the absence of PTC, we can see no benefit in using the VDF approximation with high numbers of nodes. As in the case of a hyperbolic flow with low inertia particles, two- and three-point approximations (MOM-2, MOM-3) lead to prediction of number densities lower than those inferred from the one-point VDF (MOM-1) approximation.

5. CONCLUSIONS

The predictions of particle number density by modified versions of the CQMOM, conventional Lagrangian and fully Lagrangian approaches (FLAs) in hyperbolic and Lamb vortex flows are compared. For small Stokes numbers, no particle trajectory crossings (PTCs) occur in the hyperbolic flow and all methods predict qualitatively similar results. In the case of high Stokes numbers, single-fold PTC is observed in the flow region and the two-point quadrature approximation leads to the best agreement with both Lagrangian approaches. The three-point approximation of the VDF leads to a worse prediction than the two-point approximation. Hence, the order of approximation has to be chosen based on the characteristics of the flow. In the absence of PTC, there are no benefits to using VDF approximations with high numbers of quadrature nodes compared with the one-point approximation for Lamb vortex flow calculations. In contrast to the conventional and fully Lagrangian approaches, the CQMOM results do not capture some features of particle number density fields, including double accumulation zones in the case of Lamb vortex flow. The results predicted by the FLA are shown to be in the best agreement with the results predicted by the conventional Lagrangian approach for sufficiently large numbers of particles. Also, the FLA is shown to be the most computationally efficient approach for the cases considered in the paper.

Acknowledgments. This paper has been supported by the Kazan Federal University Strategic Academic Leadership Program ("PRIORITY-2030"), and UKRI (Grant MR/T043326/1).

REFERENCES

1. C. Chalons, R. O. Fox, M. Massot, "A multi-Gaussian quadrature method of moments for gas-particle flows in a LES framework" Proceedings of the Summer Program. Center for Turbulence Research, Stanford University, 347–358 (2010).
2. C. Chalons, R. O. Fox, F. Laurent, M. Massot, A. Vie, "Multivariate Gaussian extended quadrature method of moments for turbulent disperse multiphase flow" Multiscale Modeling and Simulation **10** (4), 1553–1583 (2017).
3. C. T. Crowe, "Review–numerical models for dilute gas-particle flows" ASME, J. of Fluids Engineering **104**, 297–303 (1982).
4. S. De Chaisemartin, L. Freret, D. Kah, F. Laurent, R. O. Fox, J. Reveillon, M. Massot, "Turbulent combustion of polydisperse evaporating sprays with droplet crossing: Eulerian modeling and validation in the infinite Knudsen limit" Proceedings of the Summer Program, Center for Turbulence Research, Stanford University, 265–276 (2008).
5. S. De Chaisemartin, L. Freret, D. Kah, F. Laurent, R. O. Fox, J. Reveillon, M. Massot, "Eulerian models for turbulent spray combustion with polydispersity and droplet crossing" Comptes Rendus Mecanique **337** (6–7), 438–448 (2009).
6. O. Desjardins, R. O. Fox, and P. Villedieu, "A quadrature-based moment method for dilute fluid-particle flows" J. of Computational Physics **227** (12), 6313–6350 (2008).
7. F. Doisneau, *Eulerian modeling and simulation of polydisperse moderately dense coalescing spray flows with nanometric-to-inertial droplets: Application to solid rocket motors, PhD Thesis, Ecole Centrale Paris* (https://tel.archives-ouvertes.fr/tel-01009896).
8. D. M. Dunn, K. D. Squires, "Modeling dilute gas-solid flows using a polykinetic moment method approach" ASME, Journal of Fluids Engineering **138** (4), 041303 (2015).
9. O. Emre, D. Kah, S. Jay, Q.-H. Tran, A. Velghe, S. De Chaisemartin, R. O. Fox, F. Laurent, and M. Massot, "Eulerian moment methods for automotive sprays" Atomization and Sprays **25** (3), 189–254 (2015).
10. R. Fan, D. L. Marchisio, R. O. Fox"Application of the direct quadrature method of moments to polydisperse gas-solid fluidized beds" Powder Technology **139** (1), 7–20 (2004).

11. R. O. Fox, “A quadrature-based third-order moment method for dilute gas-particle flows” Journal of Computational Physics **227** (12), 6313–6350 (2008).
12. R. O. Fox, F. Laurent, M. Massot, “Numerical simulation of spray coalescence in an Eulerian framework: direct quadrature method of moments and multifluid method” Journal of Computational Physics **227**, 3058–3088 (2008).
13. R. O. Fox, “Large-eddy simulation tools for multiphase flows” Annual Review of Fluid Mechanics **44**, 47–76 (2012).
14. R. O. Fox, F. Laurent,A. Vie, “Conditional hyperbolic quadrature method of moments for kinetic equations” Journal of Computational Physics **365**, 269–293 (2018).
15. A. K. Gilfanov, T. S. Zaripov, S. S. Sazhin, O. Rybdylova “An Adaptive Moment Inversion Algorithm for the Quadrature Methods of Moments in Particle Transport Modelling ” Lobachevskii Journal of Mathematics, (2022). (in press)
16. A. K. Gilfanov, S. K. Zaripov, D. V. Maklakov, “Calculation of particle concentration in the problem of aerosol aspiration into a thin-walled tube” Fluid Dynamics **44** (6), 873–881 (2010).
17. D. P. Healy, J. B. Young, “Full Lagrangian methods for calculating particle concentration fields in dilute gas-particle flows” Proceedings of the Royal Society, Series A **461** (2059), 2197–2225 (2005).
18. D. Kah, F. Laurent, L. Freret, S. De Chaisemartin, R. O. Fox, J. Reveillon, M. Massot, “Eulerian quadrature-based moment models for dilute polydisperse evaporating sprays” Flow, Turbulence and Combustion **85** (3–4), 649–676 (2010).
19. F. Laurent, M. Massot, “Multi-fluid modelling of laminar polydisperse spray flames: origin, assumptions and comparison of sectional and sampling methods” Combustion Theory and Modelling **5** (4), 537–572 (2001).
20. F. Laurent, A. Vie, C. Chalons, R. Fox, M. Massot, “A hierarchy of Eulerian models for trajectory crossing in particle-laden turbulent flows over a wide range of Stokes numbers” Annual Research Briefs, Center for Turbulence Research, Stanford University, 193–204 (2012).
21. Y. Li, O. Rybdylova, “Application of the generalised fully Lagrangian approach to simulating polydisperse gas-droplet flows” International Journal of Multiphase Flow **142**, 103716 (2021).
22. D. L. Marchisio and R. O. Fox, *Computational Models for Polydisperse Particulate and Multiphase Systems* (Cambridge University Press).
23. A. N. Osiptsov, “Mathematical modeling of dusty-gas boundary layers” Applied Mechanics Reviews **50** (6), 357–370 (1997).
24. A. N. Osiptsov, “Lagrangian modelling of dust admixture in gas flows” Astrophysics and Space Science **274** (1–2), 377–386 (2000).
25. A. Papoutsakis, O. D. Rybdylova, T.S. Zaripov, L. Danaila, A. N. Osiptsov, S. S. Sazhin, “Modelling of the evolution of a droplet cloud in a turbulent flow” International Journal of Multiphase Flow **104**, 233–257 (2018).
26. F. A. Williams, “Spray combustion and atomization” Physics of Fluids **1** (6), 541–545 (1965).
27. C. Yuan, R. .O. Fox, “Conditional quadrature method of moments for kinetic equations” Journal of Computational Physics **230** (22), 8216–8246 (2011).
28. C. Yuan, F. Laurent, R. .O. Fox, “An extended quadrature method of moments for population balance equations” Journal of Aerosol Science **51**, 1–23 (2012).
29. T. S. Zaripov, A. K. Gilfanov, S. Begg, O. Rybdylova, S. S. Sazhin, M. R. Heikal, “The fully Lagrangian approach to the analysis of particle/droplet dynamics: implementation into ANSYS Fluent and application to gasoline sprays” Atomization and Sprays **27** (6), 493–10 (2017).